Structures and relative stabilities of hydrated ferrous ion clusters and temperatures effects

(Supporting information)

Ousman Boukar[a], Jean Jules Fifen[*,b], Nsangou Mama[a], Hassen Ghalila[c] and Jeanet Conradie[d]

[a]Department of Physics, Faculty of Science, University of Maroua, P. O. Box 46, Maroua Cameroon

[b]Department of Physics, Faculty of Science, University of Ngaoundere, P.O.BOX 454, Ngaoundere, Cameroon.

[c]Faculty of Science, University of Tunis El Manar, PO Box 2092, Tunis, Tunisia

[d]Department of Chemistry, University of the Free State, PO Box 339, Bloemfontein, 9300, South Africa

Content

List of figures

List of Tables

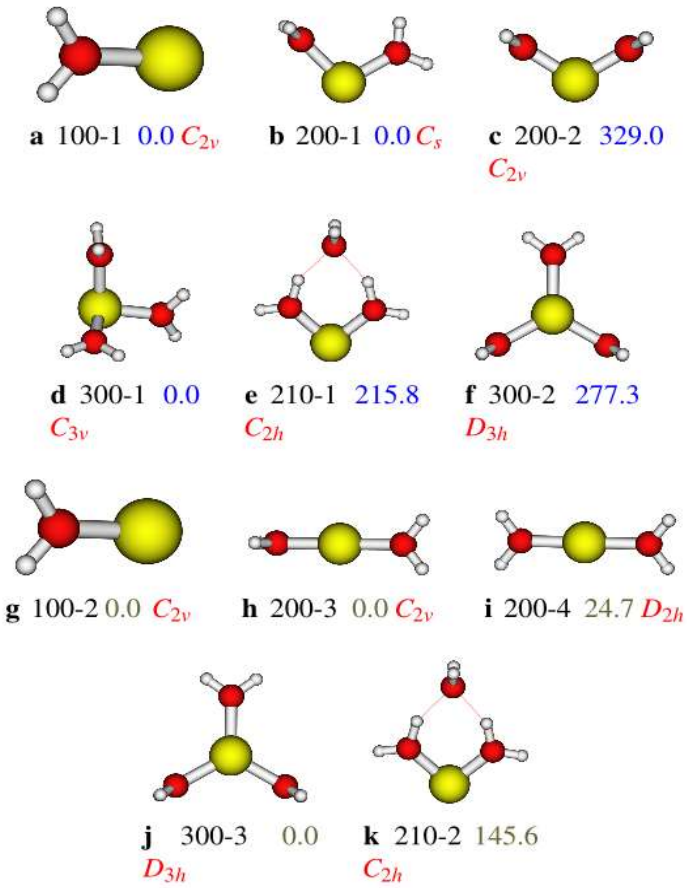

Figure 1s : Gas-phase structures of $\mathbf{Fe^{2+}(H_2O)_{n=1-3}}$ clusters.

Numbers in blue represent the zero-point-corrected relative electronic energies (ZEE) of isomers in the singlet spin-state. Numbers in gray color represent the ZEE of isomers in the quintet spin. All these numbers are in kJ/mol. Symmetry point group of each structure is indicated in red when different from $\boldsymbol{C_1}$. It should be noted here that for each figure, we first present the singlet spin state structures and then the quintet spin state ones. The high energy gaps between various isomers of a given cluster favor the global minimum ZEE structure to be the most stable at all temperatures in both spin states. Note also that structures **200-4**, **210-1**, **210-2** and **300-2** are presented here to the cluster community for the first time.

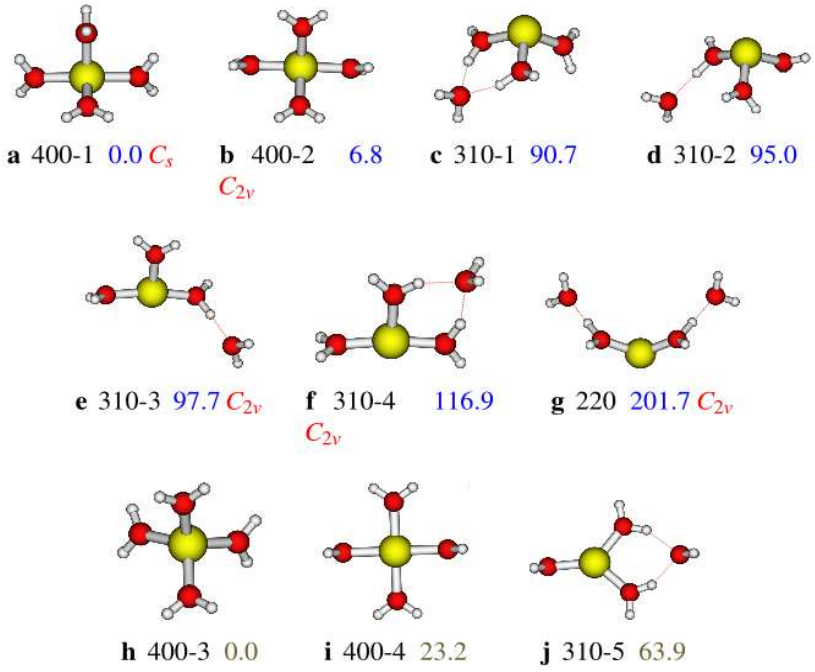

Figure 2s : Gas-phase structures of $\mathbf{Fe^{2+}(H_2O)_{n=4}}$ clusters.

See the caption of **Figure 1s** for definitions of terms. Singlet spin state results are presented through structures in **a** to **g** while quintet spin state geometries are presented by structures in **h**, **i** and **j**. As the relative energies between isomers are high in the quintet spin state, we can anticipate that the global minimum ZEE structure (**400-3**) dominates the population at all temperatures. In regard of the small ZEE between **400-1** and **400-2** as compared to other isomers in the lowest spin state, we expect a strong competition between these isomers as the temperature increases. Note also that all the structures are presented here to the cluster community for the first time, except the global minimum ZEE structure for each spin state (**400-1** and **400-3**, respectively)

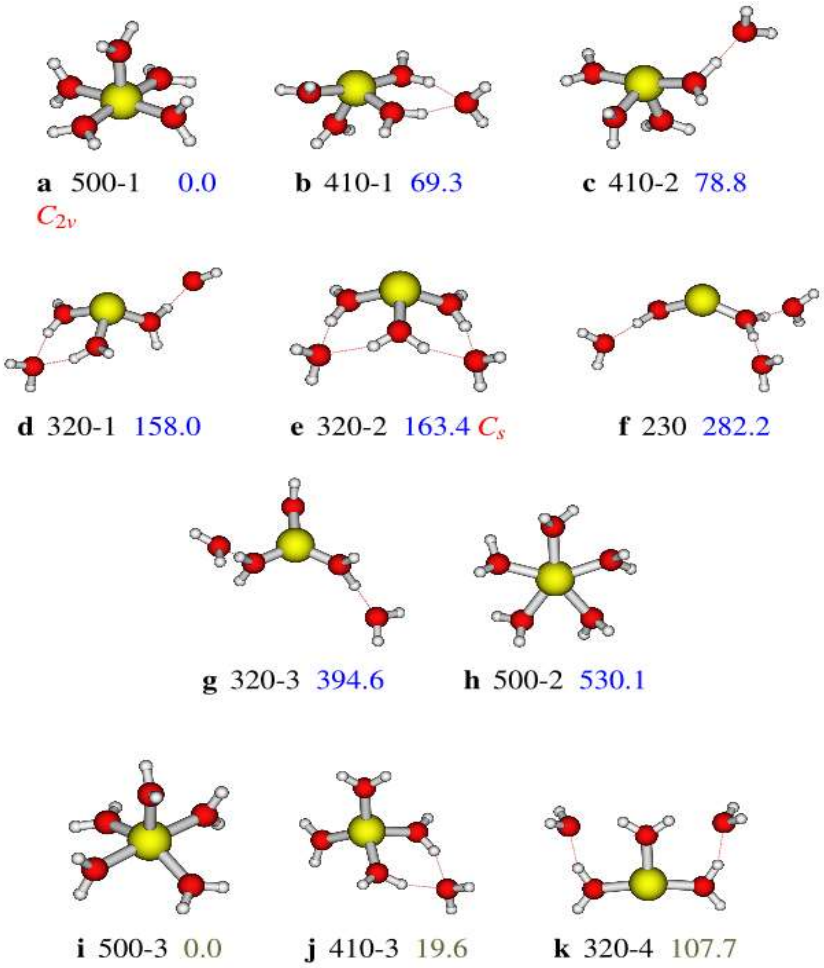

Figure 3s : Gas-phase structures $\mathbf{Fe^{2+}(H_2O)_{n=5}}$ clusters.

See the caption of **Figure 1s** for definitions of terms. Singlet spin state results are presented through structures in **a** to **h** while quintet spin state geometries are presented by structures in **i**, **j** and **k**. As the relative energies between isomers are very high in both spin state, we can anticipate that the global minimum ZEE structure for each spin state will dominate exclusively the population at all temperatures. Note also that all the structures are presented here to the cluster community for the first time, except the global minimum ZEE structure for each spin state (**500-1** and **500-3**, respectively).

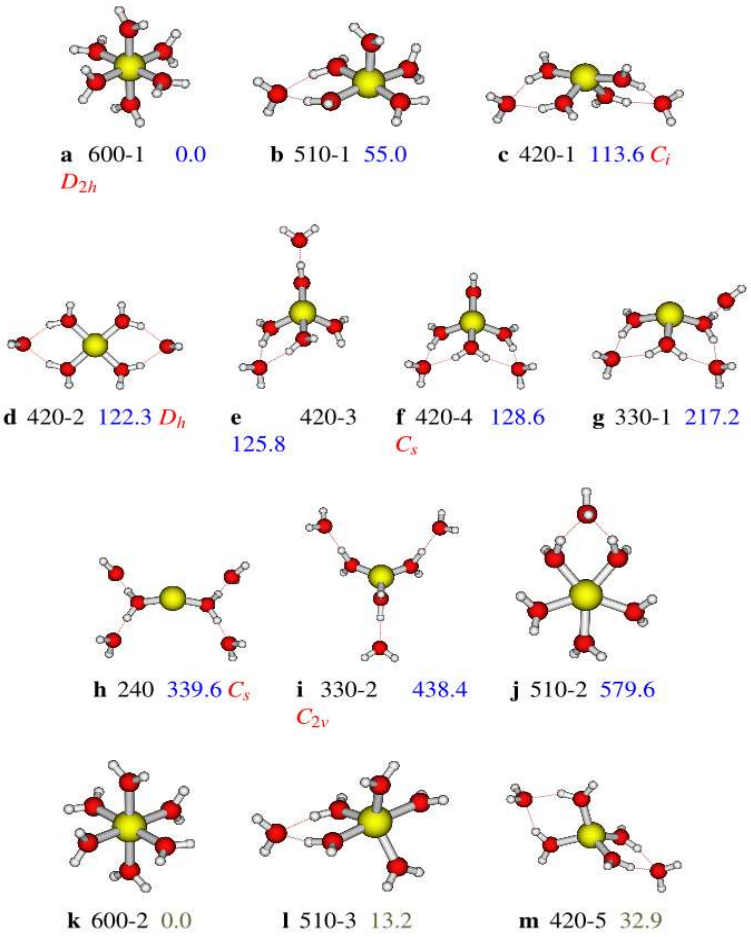

Figure 4s : Gas-phase structures of $\mathbf{Fe^{2+}(H_2O)_{n=6}}$ clusters.

See the caption of **Figure 1s** for definitions of terms. Singlet spin state results are presented through structures in **a** to **j** while quintet spin state geometries are presented by structures in **k**, **l** and **m**. As the relative energies between isomers are very high in both spin state, we can anticipate that the global minimum ZEE structure for each spin state will dominate exclusively the population at all temperatures. Note also that all the structures are presented here to the cluster community for the first time, except the global minimum ZEE structure for each spin state (**600-1** and **600-2**, respectively).

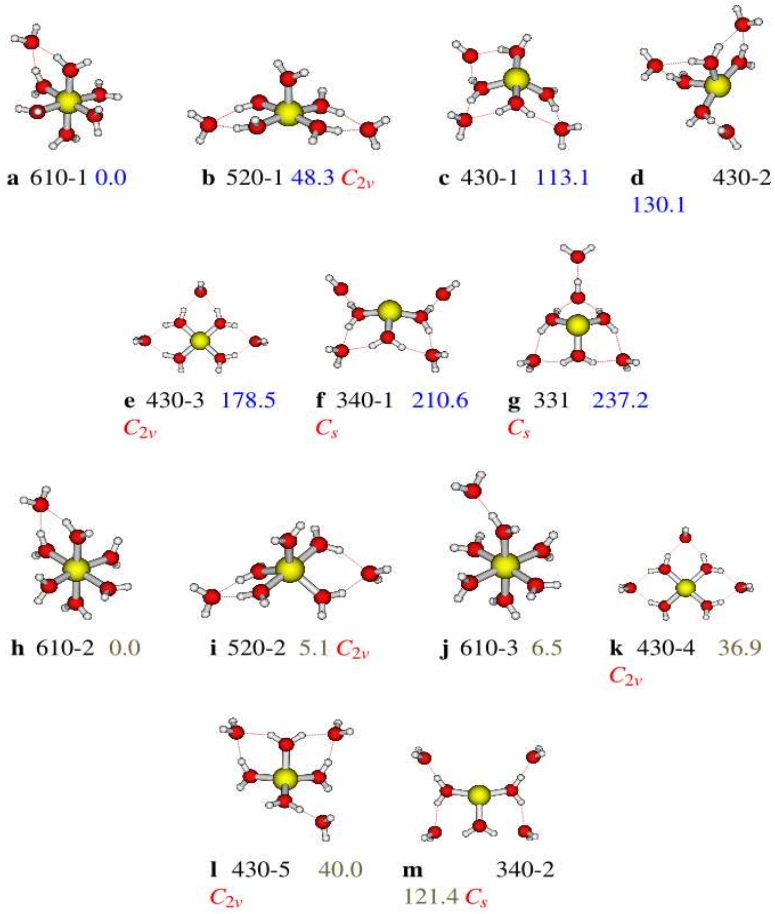

Figure 5s : Gas-phase structures of $\mathbf{Fe^{2+}(H_2O)_{n=7}}$ clusters.

See the caption of **Figure 1s** for definitions of terms. Singlet spin state results are presented through structures in **a** to **g** while quintet spin state geometries are presented by structures in **h**, to **m**. As the relative energies between the first four isomers are close in both spin state, we can anticipate a strong competition of these structures in the population of the heptamer at high temperature. Note also that all the structures are presented here to the cluster community for the first time, except the global minimum ZEE structure in the quintet spin state (**610-1**)

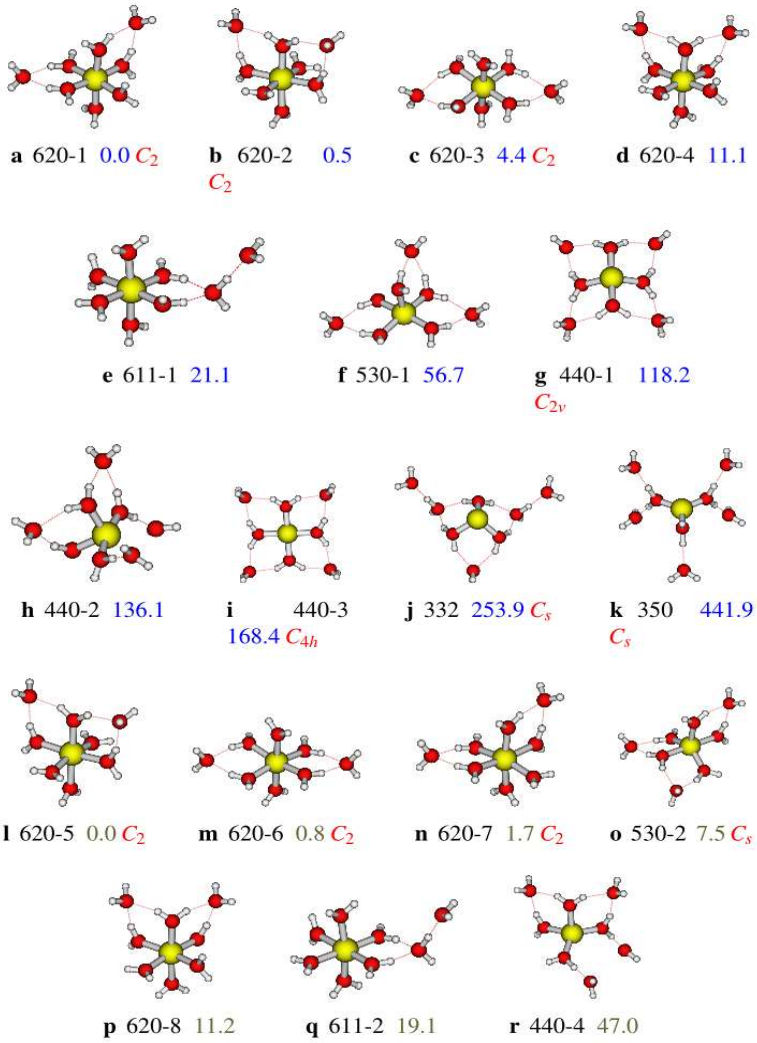

Figure 6s : Gas-phase structures of $\mathbf{Fe^{2+}(H_2O)_{n=8}}$ clusters.

See the caption **Figure 1s** for definitions of terms. Singlet spin state results are presented through structures in **a** to **k** while quintet spin state geometries are presented by structures in **l**, to **r**. As the relative energies between the first four isomers are close in both spin states, we can anticipate a strong competition of these structures in the population of the octamer at high temperature. Note also that all the structures are presented here to the cluster community for the first time, except **620-5** and **620-6**.

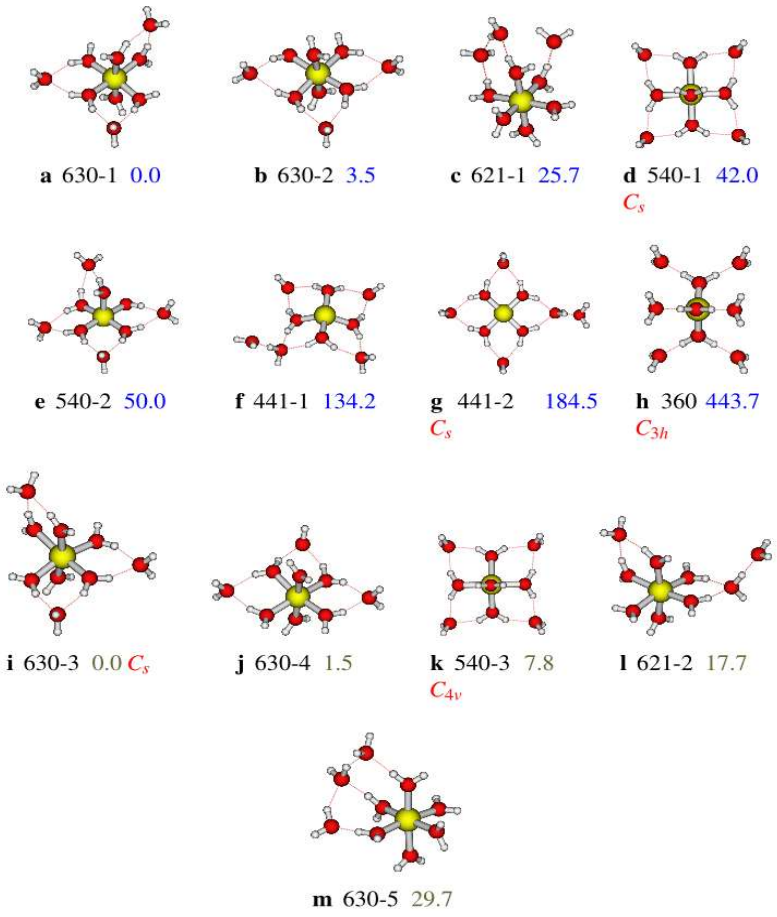

Figure 7s : Gas-phase structures of $\mathbf{Fe^{2+}(H_2O)_{n=9}}$ clusters.

See the caption **Figure 1s** for definitions of terms. Singlet spin state results are presented through structures in **a** to **h** while quintet spin state geometries are presented by structures in **i** to **m**. As the relative energies between the first three isomers are close in both spin state, we can anticipate a strong competition of these structures in the population of the nonamer at high temperature. Note also that all the structures are presented here to the cluster community for the first time, except the global minimum ZEE in the quintet spin state (**630-3**).

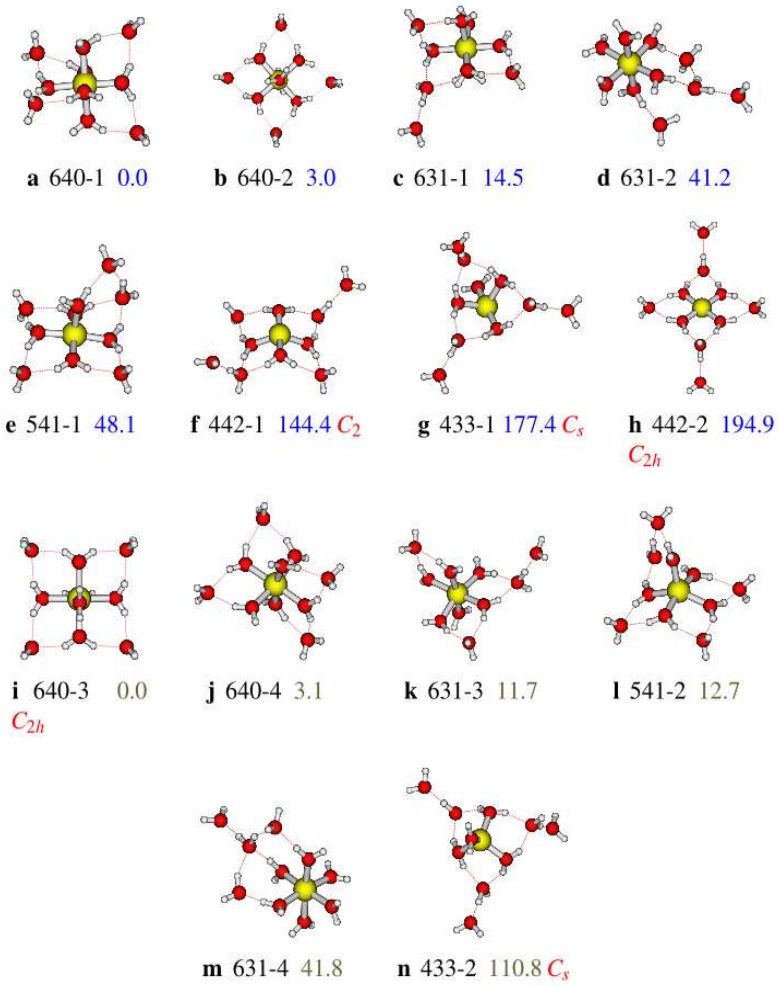

Figure 8s : Gas-phase structures of $\mathbf{Fe^{2+}(H_2O)_{n=10}}$ clusters.

See the caption of **Figure 1s** for definitions of terms. Singlet spin state results are presented through structures in **a** to **h** while quintet spin state geometries are presented by structures in **i**, to **n**. As the relative energies between the first tree isomers are close in both spin state, we can anticipate a strong competition of these structures in the population of the decamer at high temperature. Note also that all the structures are presented here to the cluster community for the first time, except **640-4**, which is not the global minimum ZEE structure.

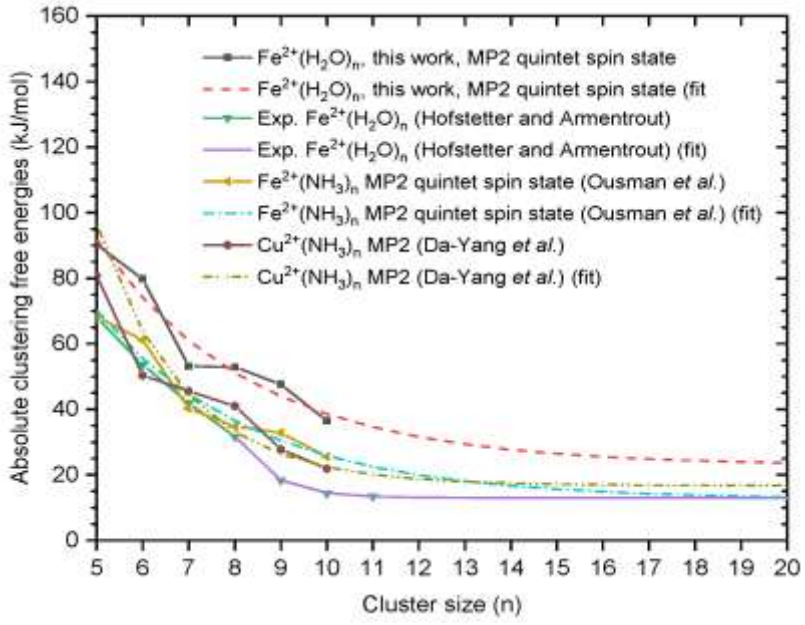

Figure 9s : Gas phase clustering energies of $Fe^{2+}(H_2O)_n$, $Fe^{2+}(NH_3)_n$ and $Cu^{2+}(H_2O)_n$ complex.

Absolute clustering free energies of complexes $Fe^{2+}(H_2O)_n$, $Fe^{2+}(NH_3)_n$ and $Cu^{2+}(H_2O)_n$. The experimental clustering free energies of the complex have been excellently extrapolated by the function $\boldsymbol{n \in N^* \mapsto A_1 \exp\left(-\frac{n}{B_1}\right) + C_1}$. with the parameters $(\boldsymbol{A_1, B_1, C_1})$ optimized to $(\boldsymbol{409410.27, 0.80, 12.98})$. Our previously calculated clustering free energies of the cluster $Fe^{2+}(NH_3)_n$ at the MP2/6-31++G(d,p) level of theory can be excellently reproduced or extrapolated by the function $\boldsymbol{n \in N^* \mapsto A_2 \exp\left(-\frac{n}{B_2}\right) + C_2}$. with the parameters $(\boldsymbol{A_2, B_2, C_2})$ optimized to $(\boldsymbol{248.7005, 3.4162, 12.5396})$. The associated root mean square error and the correlation coefficient between the fitted and the calculated clustering free energies are RMSE = 1.2 kJ/mol and $\boldsymbol{R^2 = 0.9569}$, respectively.

Our previously calculated clustering free energies of the cluster $Cu^{2+}(NH_3)_n$ at the MP2/6-31++G(d,p) level of theory can be excellently reproduced or extrapolated by the function $\boldsymbol{n \in N^* \mapsto A_3 \exp\left(-\frac{n}{B_3}\right) + C_3}$. with the parameters $(\boldsymbol{A_3, B_3, C_3})$ optimized to (1114.8160,1.8938,16.7463). The associated correlation coefficient between the fitted and the calculated clustering free energies is $\boldsymbol{R^2 = 0.9999}$. Finally, the calculated clustering free energies of the cluster $Fe^{2+}(H_2O)_n$ can be excellently reproduced or extrapolated by the function $\boldsymbol{n \in N^* \mapsto A_4 \exp\left(-\frac{n}{B_4}\right) + C_4}$. With the parameters $(\boldsymbol{A_4, B_4, C_4})$ optimized to $(\boldsymbol{4.457 \times 10^{-2}, 3.446, 5.914})$. The associated root mean square error and the correlation coefficient between the fitted and the calculated clustering free energies are $\boldsymbol{RMSE = 3.73\ kJ/mol}$ and $\boldsymbol{R^2 = 0.944}$, respectively.

Table 1s : Relative zero-point electronic energies of all isomers presented in this work (in kJ/mol) and calculated at the MP2/6-31++G(d,p) level of theory.

Structures	Relative energies at HS	Relative energies at LS
The monomer (n=1)		
100-1	-	0.0
100-2	0.0	-
The dimer (n=2)		
200-1	-	0.0
200-2	-	329.0
200-3	0.0	
200-4	24.7	
The trimer (n=3)		
300-1	-	0.0
300-2	-	277.3
300-3	0.0	-
210-1	-	215.8
210-2	145.6	-
The tetramer (n=4)		
400-1	-	0.0
400-2	-	6.8
400-3	0.0	-
400-4	23.2	-
310-1	-	90.7
310-2	-	95.0
310-3	-	97.7
310-4	-	116.9
310-5	63.9	-
220	201.7	-
The pentamer (n=5)		
500-1	-	0.0
500-2	-	530.1

500-3	0.0	-
410-1	-	69.3
410-2	-	78.8
410-3	19.6	-
320-1	-	158.0
320-2	-	163-4
320-3	-	394.6
320-4	107.1	-
230	-	282.2
The hexamer (n=6)		
600-1	0.0	-
600-2	-	0.0
510-1	-	55.0
510-2	-	579.6
510-3	13.2	-
420-1	-	113.6
420-2	-	122.3
420-3	-	125.8
420-4	-	128.6
420-5	32.9	-
330-1	-	217.2
330-2	-	438.4
240	-	339.6
The heptamer (n=7)		
610-1	-	0.0
610-2	0.0	-
610-3	6.5	-
520-1	-	48.3
520-2	5.1	-
430-1	-	113.1
430-2	-	130.1
430-3	-	178.5
430-4	36.9	-

430-5	40.0	-
340-1	-	210.6
340-2	121.4	-
331	-	237.2
The octamer (n=8)		
620-1	-	0.0
620-2	-	0.5
620-3	-	4.4
620-4	-	11.1
620-5	0.0	-
620-6	0.8	-
620-7	1.7	-
620-8	11.2	-
611-1	-	21.1
611-2	19.1	-
530-1	-	56.7
530-2	7.5	-
440-1	-	118.2
440-2	-	136.1
440-3	-	168.4
440-4	47.0	-
332	-	253.9
350	-	441.9
The nonamer (n=9)		
630-1	-	0.0
630-2	-	3.5
630-3	0.0	-
630-4	1.5	-
630-5	29.7	-
621-1	-	25.7
621-2	17.1	-
540-1	-	42.0
540-2	-	50.0

540-3	7.8	-
441-1	-	134.2
441-2	-	184.5
360	-	443.7
The decamer (n=10)		
640-1	-	0.0
640-2	-	3.0
640-3	0.0	-
640-4	3.1	-
631-1	-	14.5
631-2	-	41.2
631-3	11.7	-
631-4	41.8	-
541-1	-	48.1
541-2	12.7	-
442-1	-	144.4
442-2	-	194.9
433-1	-	177.4
433.2	110.8	-

Table 2s : Temperature dependence of the relative free energies between the High spin state (HS) and the Low spin state (LS) of $Fe^{2+}(H_2O)_{n=1}$ (in kJ/mol). Calculations are performed at MP2-6-31++G(d,p) level of theory

Temperature (K)	100_1	100_2
1	437.0	0.00
20	437.3	0.00
40	437.5	0.00
60	437.8	0.00
80	438.1	0.00
100	438.4	0.00
120	438.6	0.00
140	438.9	0.00
160	439.2	0.00
180	439.5	0.00
200	439.7	0.00
220	440.0	0.00
240	440.3	0.00
260	440.6	0.00
280	440.9	0.00
300	441.2	0.00
320	441.5	0.00
340	441.8	0.00
360	442.1	0.00
380	442.4	0.00
400	442.7	0.00

Table 3s : Temperature dependence of the relative free energies between the High spin state (HS) and the Low spin state (LS) of $Fe^{2+}(H_2O)_{n=2}$ (in kJ/mol). Calculations are performed at MP2-6-31++G(d,p) level of theory

Temperature (K)	200_1	200_3
1	443.4	0.00
20	443.5	0.00
40	443.6	0.00
60	443.8	0.00
80	444.1	0.00
100	444.5	0.00
120	444.8	0.00
140	445.2	0.00
160	445.7	0.00
180	446.1	0.00
200	446.5	0.00
220	447.0	0.00
240	447.5	0.00
260	447.9	0.00
280	448.4	0.00
300	448.9	0.00
320	449.4	0.00
340	449.9	0.00
360	450.3	0.00
380	450.8	0.00
400	451.3	0.00

Table 4s : Temperature dependence of the relative free energies between the High spin state (HS) and the Low spin state (LS) of $Fe^{2+}(H_2O)_{n=3}$ (in kJ/mol). Calculations are performed at MP2-6-31++G(d,p) level of theory

Temperature (K)	300_1	300_3
1	368.3	0.00
20	368.6	0.00
40	369.0	0.00
60	369.5	0.00
80	370.1	0.00
100	370.7	0.00
120	371.4	0.00
140	372.1	0.00
160	372.7	0.00
180	373.4	0.00
200	374.1	0.00
220	374.8	0.00
240	375.5	0.00
260	376.2	0.00
280	376.9	0.00
300	377.7	0.00
320	378.4	0.00
340	379.1	0.00
360	379.8	0.00
380	380.6	0.00
400	381.3	0.00

Table 5s : Temperature dependence of the relative free energies between the High spin state (HS) and the Low spin state (LS) of $Fe^{2+}(H_2O)_{n=4}$ (in kJ/mol). Calculations are performed at MP2-6-31++G(d,p) level of theory

Temperature (K)	**400-1**	**400-3**
1	335.7	0.00
20	336.0	0.00
40	336.4	0.00
60	336.9	0.00
80	337.6	0.00
100	338.3	0.00
120	339.1	0.00
140	340.0	0.00
160	340.8	0.00
180	341.7	0.00
200	342.6	0.00
220	343.5	0.00
240	344.4	0.00
260	345.4	0.00
280	346.3	0.00
300	347.2	0.00
320	348.2	0.00
340	349.1	0.00
360	350.1	0.00
380	351.1	0.00
400	352.0	0.00

Table 6s : Temperature dependence of the relative free energies between the High spin state (HS) and the Low spin state (LS) of $Fe^{2+}(H_2O)_{n=5}$ (in kJ/mol). Calculations are performed at MP2-6-31++G(d,p) level of theory

Temperature (K)	**500-1**	**500-3**
1	279.9	0.00
20	280.2	0.00
40	280.4	0.00
60	280.7	0.00
80	281.1	0.00
100	281.4	0.00
120	281.8	0.00
140	282.3	0.00
160	282.7	0.00
180	283.2	0.00
200	283.7	0.00
220	284.2	0.00
240	284.7	0.00
260	285.3	0.00
280	285.8	0.00
300	286.3	0.00
320	286.9	0.00
340	287.5	0.00
360	288.0	0.00
380	288.6	0.00
400	289.2	0.00

Table 7s : Temperature dependence of the relative free energies between the High spin state (HS) and the Low spin state (LS) of $Fe^{2+}(H_2O)_{n=6}$ (in kJ/mol). Calculations are performed at MP2-6-31++G(d,p) level of theory

Temperature (K)	**600-1**	**600-2**
1	240.0	0.00
20	240.3	0.00
40	240.7	0.00
60	241.3	0.00
80	242.0	0.00
100	242.9	0.00
120	244.0	0.00
140	245.1	0.00
160	246.2	0.00
180	247.5	0.00
200	248.8	0.00
220	250.1	0.00
240	251.4	0.00
260	252.8	0.00
280	254.3	0.00
300	255.7	0.00
320	257.1	0.00
340	258.6	0.00
360	260.1	0.00
380	261.6	0.00
400	263.1	0.00

Table 8s : Temperature dependence of the relative free energies between the High spin state (HS) and the Low spin state (LS) of $Fe^{2+}(H_2O)_{n=7}$ (in kJ/mol). Calculations are performed at MP2-6-31++G(d,p) level of theory

Temperature (K)	**610-1**	**610-2**	**610-3**
1	240.8	0.0	6.5
20	241.1	0.0	6.4
40	241.4	0.0	6.1
60	241.9	0.0	5.6
80	242.5	0.0	5.0
100	243.3	0.0	4.3
120	244.1	0.0	3.6
140	245.1	0.0	2.9
160	246.1	0.0	2.1
180	247.1	0.0	1.3
200	248.2	0.0	0.4
220	249.8	0.4	0.0
240	251.9	1.3	0.0
260	254.0	2.2	0.0
280	256.1	3.1	0.0
300	258.3	4.0	0.0
320	260.5	4.9	0.0
340	262.7	5.8	0.0
360	264.9	6.8	0.0
380	267.2	7.7	0.0
400	269.4	8.6	0.0

Table 9s : Temperature dependence of the relative free energies between the High spin state (HS) and the Low spin state (LS) of $Fe^{2+}(H_2O)_{n=8}$ (in kJ/mol). Calculations are performed at MP2-6-31++G(d,p) level of theory

Temperature (K)	**620-1**	**620-2**	**620-5**
1	237.5	238.0	0.0
20	237.7	238.3	0.0
40	238.2	238.7	0.0
60	238.8	239.2	0.0
80	239.6	240.0	0.0
100	240.6	240.9	0.0
120	241.7	241.9	0.0
140	242.9	242.9	0.0
160	244.2	244.1	0.0
180	245.6	245.3	0.0
200	247.1	246.6	0.0
220	248.6	247.9	0.0
240	250.1	249.3	0.0
260	251.7	250.7	0.0
280	253.4	252.1	0.0
300	255.0	253.5	0.0
320	256.7	255.0	0.0
340	258.4	256.5	0.0
360	260.1	258.0	0.0
380	261.8	259.5	0.0
400	263.6	261.0	0.0

Table 10s : Temperature dependence of the relative free energies between the High spin state (HS) and the Low spin state (LS) of $Fe^{2+}(H_2O)_{n=9}$ (in kJ/mol). Calculations are performed at MP2-6-31++G(d,p) level of theory

Temperature (K)	**630-1**	**630-3**
1	234.8	0.0
20	235.1	0.0
40	235.6	0.0
60	236.3	0.0
80	237.2	0.0
100	238.2	0.0
120	239.2	0.0
140	240.4	0.0
160	241.7	0.0
180	243.0	0.0
200	244.3	0.0
220	245.7	0.0
240	247.2	0.0
260	248.6	0.0
280	250.1	0.0
300	251.6	0.0
320	253.1	0.0
340	254.7	0.0
360	256.2	0.0
380	257.8	0.0
400	259.4	0.0

Table 11s : Temperature dependence of the relative free energies between the High spin state (HS) and the Low spin state (LS) of $Fe^{2+}(H_2O)_{n=10}$ (in kJ/mol). Calculations are performed at MP2-6-31++G(d,p) level of theory

Temperature (K)	640-1	640-2	640-3	640-4
1	231.2	234.1	0.0	3.1
20	231.5	234.4	0.0	3.0
40	231.9	234.8	0.0	2.8
60	232.5	235.4	0.0	2.6
80	233.3	236.1	0.0	2.3
100	234.3	236.9	0.0	2.1
120	235.5	237.9	0.0	1.8
140	236.7	239.0	0.0	1.6
160	238.1	240.1	0.0	1.3
180	239.5	241.3	0.0	1.1
200	241.0	242.6	0.0	0.8
220	242.5	243.9	0.0	0.6
240	244.2	245.3	0.0	0.3
260	245.8	246.7	0.0	0.1
280	247.7	248.3	0.2	0.0
300	249.6	250.0	0.4	0.0
320	251.6	251.7	0.7	0.0
340	253.7	253.5	0.9	0.0
360	255.7	255.3	1.1	0.0
380	257.8	257.0	1.4	0.0
400	259.8	258.8	1.6	0.0